THE PENNSYLVANIA STATE UNIVERSITY
SCHREYER HONORS COLLEGE

DEPARTMENT OF NUCLEAR ENGINEERING

Viability of a Cryogenic Irradiation Facility at the Penn State Breazeale Reactor

CASEY EMLER
SPRING 2022

A thesis
submitted in partial fulfillment
of the requirements
for a baccalaureate degree
in Nuclear Engineering
with honors in Nuclear Engineering

Reviewed and approved* by the following:

Jeffrey Geuther
Associate Director for Operations and Associate Research Professor of Nuclear Engineering
Thesis Supervisor

Elia Merzari
Associate Professor of Nuclear Engineering
Honors Adviser

* Electronic approvals are on file.

ABSTRACT

Penn State's Breazeale Nuclear Reactor contains a variety of dry tubes and fixtures used for irradiation experiments. The reactor currently does not have the capability of performing cryogenic irradiation testing. A cryogenic irradiation facility is desired for low-temperature irradiation testing of material specimens for various applications. In this thesis, the viability of a cryogenic irradiation facility at the Breazeale Nuclear Reactor was investigated. It was determined that an irradiation rig, placed within the fast neutron irradiation tube, was the most promising method. The rig will be cooled via a liquid nitrogen pumping system and heat transfer will be mitigated through a combination of multi-layer insulation and a vacuum pumping system. An MCNP model of the core was used to estimate gamma heating within the rig. After performing a simplified heat transfer analysis, it was determined that reactor pool water would not freeze during operation. Low temperature irradiation testing of materials was therefore found to be feasible at the facility.

TABLE OF CONTENTS

LIST OF FIGURES

LIST OF TABLES

ACKNOWLEDGEMENTS

I would like to thank Dr. Jeffrey Geuther for his guidance and support throughout the entirety of this project. Without his support, this work would not have been possible. I would also like to thank Brayden Bowie for holding me accountable during the writing process and ensuring my deadlines were met.

Chapter 1

Introduction

1.1 Purpose and Objective

The purpose of this research is to investigate the feasibility of a cryogenic irradiation facility at Penn State's Radiation Science and Engineering Center. The successful realization of this facility would enable important data to be collected on material irradiations at cryogenic temperatures. The objective of this project was to design an irradiation rig for use inside the fast neutron irradiation tube. The rig must be kept at cryogenic temperatures while not causing reactor pool water to freeze. This must all be accomplished while maximizing the material sample size that can be loaded into the rig for irradiation.

1.2 Related Facilities

To date, there have only been a handful of cryogenic irradiation facilities in the world. NASA (National Aeronautics and Space Administration) operated the first irradiation system for cryogenic experiments at the Lewis Research Center in Sandusky, Ohio [1]. The center housed the 60 MW Plum Brook Reactor which was shut down in 1973. While in operation, the facility provided invaluable data on how materials would react to the cryogenic temperatures and harsh radiation fields common during space flight.

The cryogenic irradiation facility at Plum Brook utilized a horizontal through hole which traversed the reactor pool on the north side of the reactor. The through hole was an aluminum

cylinder with an inside diameter of 11.75 inches that was cooled by circulating primary water. At full reactor power, an approximate fast neutron flux of $5.6x10^{12}$ neutrons/cm^2s was achieved inside the tube. The experimental capsule used controlled the flow of cryogenic and actuation gas to the sample and had the capability of maintaining a vacuum environment of approximately 2 microns of mercury. Currently, there are only three cryogenic neutron irradiation facilities in the world located at the Kyoto University Research Reactor Institute (KURRI), Grenoble SARA facility, and the Ohio State University Research Reactor (OSURR).

The Kyoto University Research Reactor has a cryogenic irradiation facility co-located with the reactor core. Samples loaded into the irradiation system are cooled down to 10 Kelvin by a helium gas loop and then irradiated at 1 MW with a corresponding fast neutron flux of $1.4x10^{11}$ neutrons/cm^2s [2]. The cryogenic liquid supply loop allows the samples to be irradiated for a 45-hour cycle.

The Grenoble SARA facility, dedicated to Large Hadron Collider research, is located in Grenoble, France. A liquid argon cooled cryostat is placed behind a neutron source of 6 MeV maximum energy. Neutrons are produced via a 20 MeV deuteron beam that collides with a 3-millimeter-thick beryllium target, undergoing the $^{9}Be(d,n)^{10}Be$ stripping reaction [3]. Fast neutron fluences of up to $4x10^{14}$ neutrons/cm^2s can be achieved with neutrons accounting for approximately 78% of the radiation dose (gamma dose accounting for the remainder).

The Cryogenic Irradiation Facility (CRIF) located at OSURR is the most similar research facility to the one desired at the PSBR. It is also currently the only cryogenic radiation research facility in the United Sates. The CRIF makes use of a 10-inch dry tube located adjacent to the 500 kW OSURR open pool reactor. At 450 kW, the fast neutron flux inside the dry tube is $3.6x10^{11}$ neutrons/cm^2s. The CRIF facility preloads cryogen into the cryostat and has the

capability to accommodate either liquid helium or liquid nitrogen. The sample is submerged in the liquid cryogen bath for experimentation. Using Monte Carlo N-Particle (MCNP6) simulations, it was conservatively estimated that the reactor could operate at 15 kW for 6.66 hours before total boil-off occurs [4].

1.3 Applications

1.3.1 Aerospace Research

A cryogenic irradiation radiation facility at the PSBR will allow for a variety of research in multiple disciplines. With the Plum Brook irradiation facility closed, there is a need for materials testing for space travel. Spacecraft such as satellites, rovers, and probes are placed under extremely harsh environments when launched into space. The spacecraft themselves, and the important equipment onboard, are exposed to temperatures just above absolute zero. In addition to temperature concerns, the materials are also exposed to numerous forms of high energy radiation from sources such as galactic cosmic rays and solar particle events. Without Earth's protective atmospheric shielding, the effect this radiation has on certain materials is not completely understood. By understanding how the combination of radiation damage and extremely low temperatures affect materials, spacecraft can be better optimized for travel.

In addition to background radiation, NASA and the private industry have renewed interest in nuclear thermal propulsion (NTP). NTP rockets operate similar to traditional chemical rockets but utilize nuclear fission heat instead of combustion as a propulsion source. NTP concepts have been researched since the 1950's due to high specific impulse they offer (thus significantly reducing round trip travel times). Concepts such as the centrifugal nuclear thermal

rocket have the capability to outperform the best available chemical in-space engines by a factor of four [5].

These proposed methods of propulsion produce mixed radiation fields that can be detrimental to the structural integrity of the spacecraft as well as the electronics and communications systems onboard. High energy neutrons are a main source of this damage as they create collision cascades that produce microstructural changes in the material such as point defects and dislocations. Understanding how the materials respond under this complex environment is pivotal to the success of a deep space mission utilizing NTP technology.

1.3.2 Fusion Research

In addition to space-based research, the irradiation of materials at cryogenic temperatures is important for other applications such as nuclear fusion materials research. The most heavily researched reaction for fusion energy is the $t(d,n)^3He$ reaction. A plasma temperature of approximately $2x10^8$ K is required for this reaction to occur by overcoming the coulomb repulsion between the deuteron and triton [6].

Fusion reactors offer unique radiation challenges as temperatures in structural materials range from cryogenic temperatures to above 1270 K in more exposed regions. Due to the extreme heat created by the plasma, cryogenic technology is extensively used in fusion reactors such as ITER to maintain low-temperature conditions for the massive magnet system. In order to confine and stabilize the plasma, high magnetic fields are necessary which requires the magnets to be cooled with liquid helium.

Combined with the extreme temperatures, 14.1 MeV fusion neutrons are released from the $t(d,n)^3He$ reaction. Fusion neutrons are like fission neutrons in that they gradually slow down in materials and subsequently lose their energy by creating displacement defects and heat [6]. Unlike fission neutrons, fusion neutrons can create gaseous and solid transmutation products which can cause displacement damage. Although this effect cannot be seen with fission neutrons, attempts at correlating this degradation have been made [7]. A cryogenic irradiation facility at the PSBR could provide critical materials research for the cryogenic environments of fusion reactors.

1.3.3 Superconductor Research

A semiconductor is a material that has an electrical conductivity value falling between that of a conductor and an insulator. A semiconductor has an electronic band structure that exhibits a gap between the valence and conduction bands. As temperature increases, the energy gap between the conduction band and valence band decreases. Conversely, as temperature decreases, there are less charge carriers at lower temperatures which increases the resistivity of the semiconductor.

A semiconductor is enhanced by doping it with donor or acceptor impurities. This change in the electronic band structure either increases or decreases the conductivity of the material. Semiconductors have traditionally been used minimally within high radiation field applications due to the radiation exposure leading to degradation of key electrical parameters of the material [8]. Further study and development of semiconductors under radiation fields could yield materials that are more resistant to radiation damage.

1.3.4 Semiconductor Research

Superconductivity is a special property of certain materials to conduct electricity without energy loss when cooled to a critical temperature. In this state of matter, the material has no electrical resistance and does not allow magnetic fields to penetrate greater than a certain penetration depth which is known as the Meissner effect. When below this critical temperature, the electrons in the metal form Cooper pairs and cannot provide any electrical resistance, providing the basis for superconductivity in metals [9].

A superconductor is required anytime a strong magnetic field is being utilized such as for magnetic resonance imaging (MRI) and high-speed magnetic levitation trains. Superconductors are also critical for high energy particle accelerators and nuclear fusion reactors. The first superconducting magnet systems used for plasma experiments of a tokamak occurred in 1986 [10]. The radiation response of magnet components, such as superconducting materials, to fast neutrons is a critical parameter to the operation of these fusion reactors.

1.4 Breazeale Reactor and FNI Tube

The Penn State Breazeale Reactor is a 1 MWt, TRIGA Mark III reactor with pulsing capabilities up to 2000 MWt. The reactor contains a movable core at a depth of approximately 18 feet that is submerged in a pool of approximately 71,000 gallons of water. At steady state reactor operation of 1 MW, the fast neutron flux at the boundary of the core is $5x10^{12}$ neutrons/cm^{2}s and thermal flux is $1.3x10^{13}$ neutrons/cm^{2}s. When pulsed to 2000 MWt, fast neutron fluxes of about $1.0x10^{16}$ neutrons/cm^{2}s can be achieved. Numerous dry tubes and other fixtures are available in or near the core for experiments, one of which is the fast neutron irradiation tube (FNI).

The fast neutron irradiation tube is a stand-up pipe located adjacent to the PSBR core. The FNI dry tube has a 10” diameter is 20’ long. The tube consists of three elements: a floor-mounted shielding pedestal, top-mounted tube, and a removable shield plug. The dry tube is bolted to the shielding pedestal assembly on the bottom and braced to the pool walls on the top of the tube. The tube has an inner diameter of 10.02” and an outer diameter of 10.75”. Around the bottom 34” of the tube is an exterior rectangular cowling which encloses the shielding. The cowling also provides an airtight seal which eliminates the moderation of fast neutrons by water inside the boral absorber jacket.

The shield plug is designed to minimize radiation escaping out of the top of the FNI tube. The plug is a composite of neutron absorbing and gamma ray shielding materials that is suspended from the top of the tube. An overhead crane is used to raise and lower the shield plug into its place inside the tube.

Chapter 2

Background

2.1 Material Degradation

As discussed above, the effects of radiation fields on the properties of solids are extremely important to multiple disciplines. When radiation interacts with a solid, it can cause physical changes to the atomic-level structure. This phenomenon is known as radiation damage and can have a significant impact on the integrity and function of materials. While selecting materials to manufacture the PSBR cryogenic irradiation rig, these effects must be heavily considered. While in operation, reactor materials are exposed to intense fast neutron and gamma radiation fluxes. These radiation particles, when in contact with reactor materials, can cause lattice defects in the crystalline structure of the material. The largest contributor to radiation damage in structural materials is fast neutrons.

When considering the interaction of particle flux with a solid, it is first important to define a cross section. The probability of a reaction occurring between an incident particle and a nucleus is represented by a cross section [11]. The microscopic cross section σ represents the effective target area of a single nuclear and is measured in the unit of barns (equal to 10^{-24} cm^2).

Macroscopic cross section Σ is the probability a particle will undergo a reaction per unit length travelled in a target material. Macroscopic cross section can be derived from microscopic cross section via Equation 2.1 shown below where N is the atomic number density.

$$\Sigma = \sigma N \tag{2.1}$$

The differential probability that an incident particle will interact with a target atom in an element with thickness dx is then defined as:

$$dP = \Sigma dx \quad (2.2)$$

2.1.1 Neutron Induced Displacement Damage

The effects of radiation can be separated into two components: creation of a primary knock-on atom (PKAs) and creation of transmuted atoms [12]. Fast neutrons interacting with a solid can either elastically or inelastically scatter. The interaction between a neutron-atom scattering reaction first forms a PKA which is then followed by secondary recoils. Displacement damage is defined as removing atoms from their equilibrium lattice positions.

When an atom is struck by incident radiation, it starts a replacement collision sequence along a crystallographic direction [13]. If the initial energy of the struck atom is of a certain energy threshold, the replacement collision sequence only returns partially to the original location. At the end of the chain, a self-interstitial atom is formed, and a vacant lattice site is formed at the site of initial collision. An interstitial defect occurs when an atom occupies a normally unoccupied site in the crystalline structure. A vacancy defect is when a normally occupied lattice site is unoccupied. The combination of a self-interstitial atom and vacant lattice site is known as a Frenkel pair.

Typical energies of PKA's are on the order of keVs which is far greater than the thermal energy of material atoms which may be on the order of 10^{-2} eV [12]. Because of this difference in energy, PKAs quickly interact with surrounding atoms which in turn displace other atoms. This process initiates a displacement cascade. The characteristic features of displacement cascades are the formation of depleted zones and subcascades. Depleted zones are a region poor

in interstitial and rich in vacancy defects. Subcascades occur when the initial cascade energy is high enough to form several more cascades of defects [14].

2.1.2 Gamma Induced Displacement Damage

Gamma rays induced damage in materials via the excitation of electrons rather than directly delivering energy to the nucleus. This can occur through the photoelectric effect, Compton scattering, or pair production. These energetic electrons can go on to cause displacement damages to the material with Compton scattering being the most important of these reactions [12].

Compton scattering is the elastic scattering of a gamma ray by an electron where both energy and momentum are conserved. Unlike pair production and the photoelectric effect, the gamma ray does not disappear in the reaction [11]. This represents a unique challenge as the gamma ray is then free to interact again with other atoms in the material. The displacements per atom (dpa) rate is given by Equation 2.3 where E_γ is the gamma energy, σ_d is the displacement cross section, and $\phi(E_\gamma)$ is the specified photon spectrum.

$$k_\gamma = \int_{E_{\gamma,min}}^{\infty} \sigma_d(E_\gamma)\phi(E_\gamma)\, dE_\gamma \tag{2.3}$$

2.2 Neutron Activation

Neutron activation is the process by which neutron radiation induces radioactivity in a material due to the capture of said neutrons. The probability of a neutron capture reaction

occurring is given by the neutron capture macroscopic cross section. When the neutron has been captured, the atom becomes a new isotope with an extra neutron and additional energy. This new isotope is typically unstable and must decay to a stable state through the emission of additional radiation. When under a high neutron fluence, neutron activation can happen at a higher rate which can change material properties significantly through erosion.

Therefore, neutron activation concerns present serious challenges regarding structural integrity, maintenance, and disposal of materials [15]. Any material chosen for the irradiation rig must have a low microscopic capture cross section and/or short-lived daughter isotopes to mitigate the effects of neutron activation.

2.3 Gamma Heating

As discussed previously, gamma rays interact with materials or irradiation samples in reactors via the photoelectric effect, Compton scattering, or pair production. In the photoelectric effect, the incident gamma ray is absorbed by the atom and an energetic electron is ejected from the atom. In the pair production process, the incident gamma ray is absorbed by the atom and an electron-positron pair is created. Both the photoelectric effect and Compton scattering are inelastic interactions and can therefore increase the temperature of the material [16].

Gamma heating concerns are a critical issue in research reactor and heat deposition rates should be determined to obtain optimal irradiation of targets. Due to the significant safety concerns, gamma heating has been heavily studied globally. Lee et. al. developed a model using TRIPOLI-4 Monte Carlo code to evaluate the heating contributions from both prompt and decay

gamma factors [17]. Varvayanni et. al. developed a simple analytical model to evaluate gamma heating measurements that was verified by a numerical 3D gamma heating code [18].

2.4 Cryogenic Liquids

Cryogenics is typically regarded as the study of low-temperature materials below -150℃. Commonly used cryogenic liquids include nitrogen, helium, hydrogen, and argon. Liquid nitrogen, the cryogen to be used at the PSBR, has a normal boiling point of 77.36 K, a density of 806.1 kg/m^3, and a thermal conductivity of 0.145 W/m-K [19]. Normal boiling point is defined as the boiling point at 1 atmosphere of pressure. Liquid nitrogen is commercially manufactured relatively easily by the cryogenic distillation of liquified air.

When dealing with cryogenic liquids, heat transfer is an important concern due to the inherent extreme temperatures. Barron et. al. define the following four challenges that arise when dealing with cryogenic heat transfer that are relevant to this project [19]:

1. Effects of variable material properties. At low temperatures, the transport properties of materials vary significantly with temperature. Therefore, constant property analysis may be invalid when dealing with cryogenic applications.
2. Thermal insulation. Specially designed insulation systems are required to minimize the evaporation of cryogenic liquids due to their relatively small heat of vaporization.
3. Near-critical-point convection. Cryogenic liquids have relatively low critical pressures which means conductive heat transfer at near critical and super-critical conditions are encountered.

4. Thermal radiation problems. Peak radiant intensity wavelength is inversely proportional to absolute temperature. Metallic shields used to reduce radiation heat transfer must have a similar thickness to this wavelength value.

When dealing with the cryogenic irradiation rig, solid and gaseous conduction, convection, and radiation must be considered. Due to the cylindrical design of the FNI tube, the irradiation rig will also be cylindrical. Heat transfer consideration are imperative to ensure that reactor pool water does not freeze.

Chapter 3

Materials and Methods

3.1 Inner and Outer Cannister

The combination of cryogenic temperatures and a strong radiation field presents a unique challenge when designing an irradiation rig for use inside the PSBR. As discussed in Section 2.1, a flux of high energy particles ejects atoms from their thermodynamic equilibrium in a lattice and moves them to other places. When exposed to high fluence, this radiation can cause significant material degradation, especially at cryogenic temperatures. It has been shown that at low temperatures, only limited recombination occurs, and a large fraction of micro-damage remains in the lattice [20]. Radiation also significantly increases the creep rate within a material when compared to creep induced by thermal or other mechanisms [21].

The thermomechanical property changes of materials during irradiation are an important consideration. The structural support materials for the irradiation rig must therefore be chosen appropriately to ensure the integrity of the system under the conditions experienced within the FNI tube. For this reason, Grade 304 Stainless Steel and Aluminum 6061-T6 were considered for the inner and outer containment material.

3.1.1 Stainless Steel

Type 304 Stainless Steel is extensively used in the nuclear industry as a cladding and structural material due to its corrosion resistance and strength at a wide range of temperatures [22]. 304 is an austenitic stainless steel comprised primarily of iron, chromium, and nickel.

Chromium increases tensile strength, hardness, and resistance to corrosion. Nickel is also added to increase strength and hardness without sacrificing ductility. The effects of neutron irradiation on 304 are well studied at high fluences with the steel showing a strong resistance to material degradation against irradiation [22][23][24].

Austenitic stainless steels such as 304 are also utilized in cryogenic systems due to their mechanical properties and formability [25]. The mechanical behavior of 304 at cryogenic temperatures has been widely studied as a result and it shows excellent strength-ductility synergy without embrittlement at extremely low temperatures [26][27]. When combined with high levels of radiation, it has been shown that 304 used in cryogenics demonstrates excellent mechanical properties [21].

3.1.2 Aluminum

Aluminum 6061 is a precipitation-hardened aluminum alloy and is one of the most common alloys of aluminum due to its strength and toughness. T6 temper 6061 has been thermally treated, quenched in water, and then aged at lower temperatures to achieve a maximum precipitation hardening. This significantly increases the yield strength of the 6061 and provides excellent corrosion resistance.

Unlike stainless steel, aluminum alloys have limited use in power reactors due to temperature limitations. However, aluminum alloys have been extensively used as a structural and cladding material under the milder conditions of research and test reactors. As a result of its prevalence in industry, 6061 has shown limited post-irradiation changes in tensile properties [28][29]. It is therefore reasonable to assume that aluminum will perform adequately under the

less extreme irradiation and stresses experienced in the FNI tube (the dry tube itself is made of aluminum). Data from the now decommissioned High Flux Beam Reactor suggested that a high fast neutron flux may actually help randomize the location of silicon atoms in the alloy, reducing their negative effects on the mechanical properties of the alloy [30].

At cryogenic temperatures, diffusion processes are less pronounced and the degree of radiation hardening in 6061 will be significantly greater than room-temperature irradiation. A beneficial characteristic of low temperature irradiation, however, is that most damage anneals out when the temperature is raised. It has been shown that there is no detectable hardening of 6061 after a fast neutron irradiation of 1.4×10^{22} neutrons/m^2 at liquid nitrogen temperatures [31].

3.1.3 Material Selection

The mechanical properties under cryogenic fast neutron irradiation of both Type 304 Stainless Steel and Aluminum 6061-T6 were considered. It was determined that Aluminum 6061-T6 should be used as the structural material to manufacture the irradiation rig at the PSBR. This was due to the material's low neutron absorption cross section, good resistant to corrosion, previous dependability in research reactors, and low cost. Reinke stated that the CRIF at Ohio State utilized Al-6061 as a structural material due to its low activation, short half-lives of activated isotopes, and structural integrity under high fluence [4]. Material properties of 6061 are discussed below.

Fast neutron activation concerns in Aluminum 6061 have been previously studied due to the construction of high energy particle accelerators and lasers [32][33]. In 6061, aluminum atoms will mainly become radioactive through neutron activation via the $^{27}Al(n,\alpha)^{24}Na$ reaction.

This reaction has a half-life of 14.7 hours and gamma-decay energies of 1.38 and 2.75 MeV. Although there are other radionuclides produced, the radioactivity of Na-24 dominates. Due to its half-life of 14.7 hours, the rig should be left in the dry tube for an extended period of time to allow for this residual activity to decay to a negligible amount. Using the rule that a sample is considered safe after 10 half-lives, the rig should be left in the FNI tube for a minimum of 6 days post-shutdown to account for aluminum activation products.

For heat transfer calculation concerns, the thermal conductivity as a function of temperature is shown below in Figure 1. At liquid nitrogen temperatures of 77 K, the thermal conductivity of 6061-T6 is 83.53 W/mK. At a room temperature of 293 K, the thermal conductivity is calculated to be 154.35 W/mK. The heat generated by gamma heating in the outer cannister should be removed by the primary coolant in the reactor.

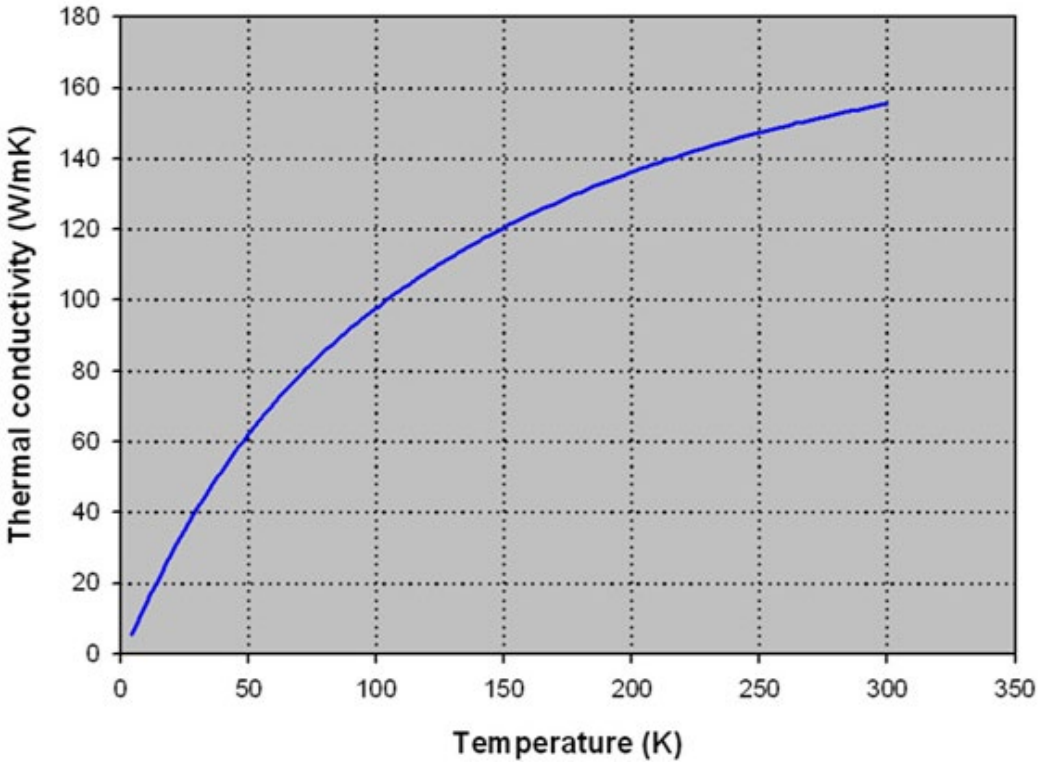

Figure 1. Thermal Conductivity of Aluminum 6061-T6 [34]

3.2 Thermal Insulation

To minimize heat transfer into and out of a system, high-performance materials are necessary for cryogenic systems. Cryogenic insulation materials are designed to provide excellent thermal insulation, all while maintaining mechanical strength under extremely cold conditions. Therefore, insulation materials must offer exceptionally low thermal conductivities while also not becoming embrittled. The necessity of an insulation system becomes increasingly complex when dealing with cryogenic liquid in the vicinity of a nuclear reactor due to boil-off concerns.

Boil-off is inherent to the storage and transfer of a cryogenic liquid due to the extreme temperature gradient between the ambient environment and the cryogen. When a cryogenic liquid heats up and reaches its boiling point, a subsequent boil-off gas is produced from the boiling liquid cryogen. Fission-generated heat from the reactor pool, combined with gamma-ray heating in the cryostat materials, could significantly increase boil-off without proper thermal insulation. Alternatively, improper thermal insulation could also lead to heat transfer through the irradiation rig and subsequent freezing of the pool water. Thus, the thermal insulation chosen for the irradiation rig must prevent these occurrences. Silica Aerogel, fiberglass, and multilayer insulation (MLI) were evaluated as thermal insulators due to their low effective thermal conductivity values.

3.2.1 Aerogel

Aerogels are solid materials characterized by an extremely low density. This is due to their dendritic grain structure with fractal chains of particles, leaving small pores throughout the

material that are in the nanometer range. The nano-porous structure combined with the high specific surface area makes aerogel a superinsulation material with very low thermal conductivity. Due to a characteristically high infrared transparency, radiant heat transfer dominates total heat transfer through the material [19]. The thermal conductivity for aerogel insulations is given by Equation 3.1 where k_0 is the thermal conductivity under a vacuum, d_1 is the mean diameter of the pores, k_g is the thermal conductivity of the gas within the aerogel, and λ is the mean free path of the gas at the mean temperature within the aerogel.

$$k_t = k_0 + \frac{k_g}{1 + 1.6\left(\frac{\lambda}{d_1}\right)} \tag{3.1}$$

For silica aerogel, silica itself is a poor conductor of heat and the small size of the pores minimizes convective heat transfer. Studies of silica aerogel have shown no ageing effects when irradiated by gamma-rays and only a moderate degradation of clarity when irradiated with a neutron fluence of 55.15×10^{12} neutrons/cm^2 [35]. Fortunately, clarity is not a concern for a thermal insulator inside an irradiation rig. The major disadvantage of silica aerogels is that they are extremely brittle and friable [36]. The large pore volume which characterizes aerogels leads to these poor mechanical properties and to combat this, aerogels can be reinforced by compositing them with other materials.

3.2.2 Fiberglass

Fiberglass is made from molten glass that is blown into extremely fine fibers. Fiberglass insulation has previously been used in in-core and near-core experiments at the PSBR and has

proven to hold up well. Fibrous materials minimize heat transfer by suppressing gaseous convection due to the small void sizes within the material. The thermal conductivity for fibrous materials is given by Equation 3.2 where Φ is the porosity and k_s is the thermal conductivity of the fibrous material.

$$k_t = \frac{k_g}{1 - (1 - \Phi)\left(1 - \frac{k_g}{k_s}\right)} \tag{3.2}$$

Fiberglass has shown no degradation of strength as a result of high neutron fluences [37][38][39]. Gamma ray irradiation has been shown to degrade strength at a fluence of 1 MGy and cause delamination at 10 MGy [39]. At cryogenic temperatures, the apparent thermal conductivity of fibrous insulation (same principle holds true for aerogel) approaches the thermal conductivity of the gas within the insulation. Evacuating the gas from the insulation is therefore one method to reduce heat transfer through the fiberglass. Evacuating fiberglass to a pressure of less than 10^{-3} torr lowers the thermal conductivity from 25 mW/m·K (ambient pressure of 760 torr) to 1.70 mW/mK [19].

3.2.3 Multilayer Insulation

Multilayer insulation is made of thin layers of highly reflective metal that act as a thermal shield around a cryogenic system. Companies such as Aerospace Fabrication and Dunmore Aerospace offer a wide variety of MLI products for various cryogenic applications. Layers of MLI are stacked on top of each other with each layer consisting of a reflective foil and spacer material. MLI is highly effective in situations where radiant heat transfer dominates. Therefore, in order to effectively insulate against thermal losses, MLI must be used under vacuum

conditions. The thermal conductivity variation for a typical MLI as a function of residual gas pressure is shown below in Figure 2. Thermal conductivity is shown to decrease by several orders of magnitude as gas is evacuated from the material.

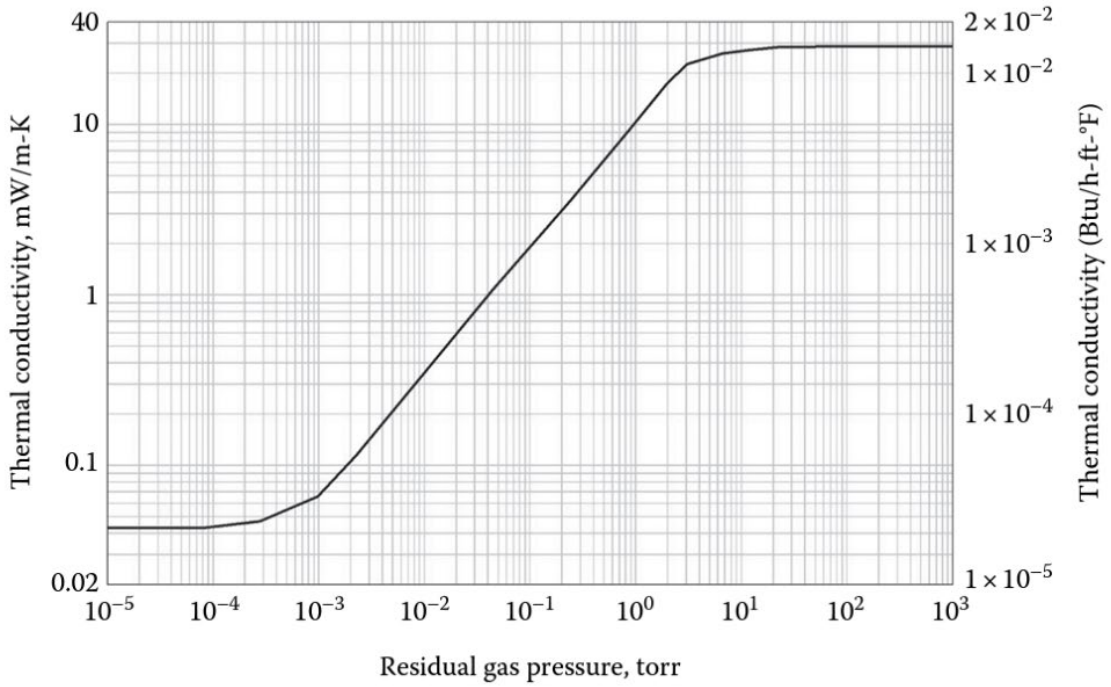

Figure 2. MLI Thermal Conductivity as a Function of Residual Gas Pressure [19]

The popularity of multilayer insulation in cryogenic systems stems from their extremely low thermal conductivities. Solid conduction is minimized by using a low-conductivity material under evacuated conditions. Due to the removal of gas within the material, both gaseous conduction and convection are virtually eliminated as heat transfer modes. Therefore, radiation is the main form of heat transfer which is combatted with multiple layers of reflective foil [19].

3.2.4 Insulation Selection

The use of thermal insulation is necessary for any cryogenic system. Insulation materials used for the irradiation rig at the PSBR must serve two critical purposes:

1. Prevent boil-off of cryogenic liquid
2. Prevent freezing of reactor pool water

While performing these tasks, the thermal insulation must also maintain structural integrity and insulation quality during intense irradiation. For this reason, it was determined that MLI should be used as the thermal insulation for the irradiation rig. MLI is the most effective thermal protection available for cryogenic systems when applied at optimal layer densities (number of layers per unit thickness). As layer density is increased, thermal conductivity decreases until a threshold value. Once this layer density has been reached, any further increase in layer density will compress the insulation too tightly and heat transfer will increase [19]. The thermal conductivity of an evacuated MLI is given by Equation 3.3 where $\frac{N}{\Delta x}$ is the layer density, h_c is the conductance of the spacer material, e is the emissivity of the reflective foil, σ is the Stefan-Boltzmann constant, and T_H and T_C are the boundary temperatures.

$$k_t = \frac{1}{\left(\frac{N}{\Delta x}\right)}\left[h_c + \left(\frac{e}{2-e}\right)\sigma(T_H^2 + T_C^2)(T_H + T_C)\right] \tag{3.3}$$

The major challenge associated with MLI usage is that parallel thermal conductivity along layers is significantly larger than perpendicular thermal conductivity [40]. MLI wrapped around the outside of the inner cannister should therefore not touch the outer cannister to minimize heat transfer out of the rig.

The effect of irradiation on MLI has been studied for space applications in NTP rockets [41][42]. MLIs have been used extensively in previous satellites and launch vehicles utilizing NTP, demonstrating their resistance to cryogenic temperatures combined with radiation flux for extended periods of time. In a feasibility study for a cryogenic irradiation facility at the Japan Materials Testing Reactor, MLI was chosen to thermally insulate vacuum jacketed transfer tubes containing helium gas at 20 K [43].

3.3 Vacuum System

Due to the use of MLI, a vacuum is needed between the inner and outer canisters to allow the MLI to perform effectively. This vacuum will also serve the dual purpose of further minimizing heat transfer between the outer layer of the MLI and inside of the outer container. Conduction and convection through the vacuum region will be essentially eliminated and the MLI will decrease radiant transfer sufficiently.

To maintain a vacuum between the concentric outer and inner canisters, a vacuum pumping system will be utilized. Companies such as Leybold and Pfeiffer offer low-cost turbo vacuum pumps capable of evacuating volumes to ultrahigh vacuums. The vacuum pump will be connected to a vacuum line which will run down the length of the FNI tube to the irradiation rig. The vacuum turbo pump line will connect to the rig top via a KF-25 t-splitter. The splitter will be inserted into a KF-25 mating flange on the top of the rig. The splitter will allow a vacuum gauge to be utilized on one of the flanges which will monitor system pressure and ensure a sufficient vacuum is maintained. This setup is shown below in Figure 3. The CRIF facility at Ohio State

utilizes this system which has proven to be effective at both maintaining a vacuum in the cryostat and minimizing heat transfer [4].

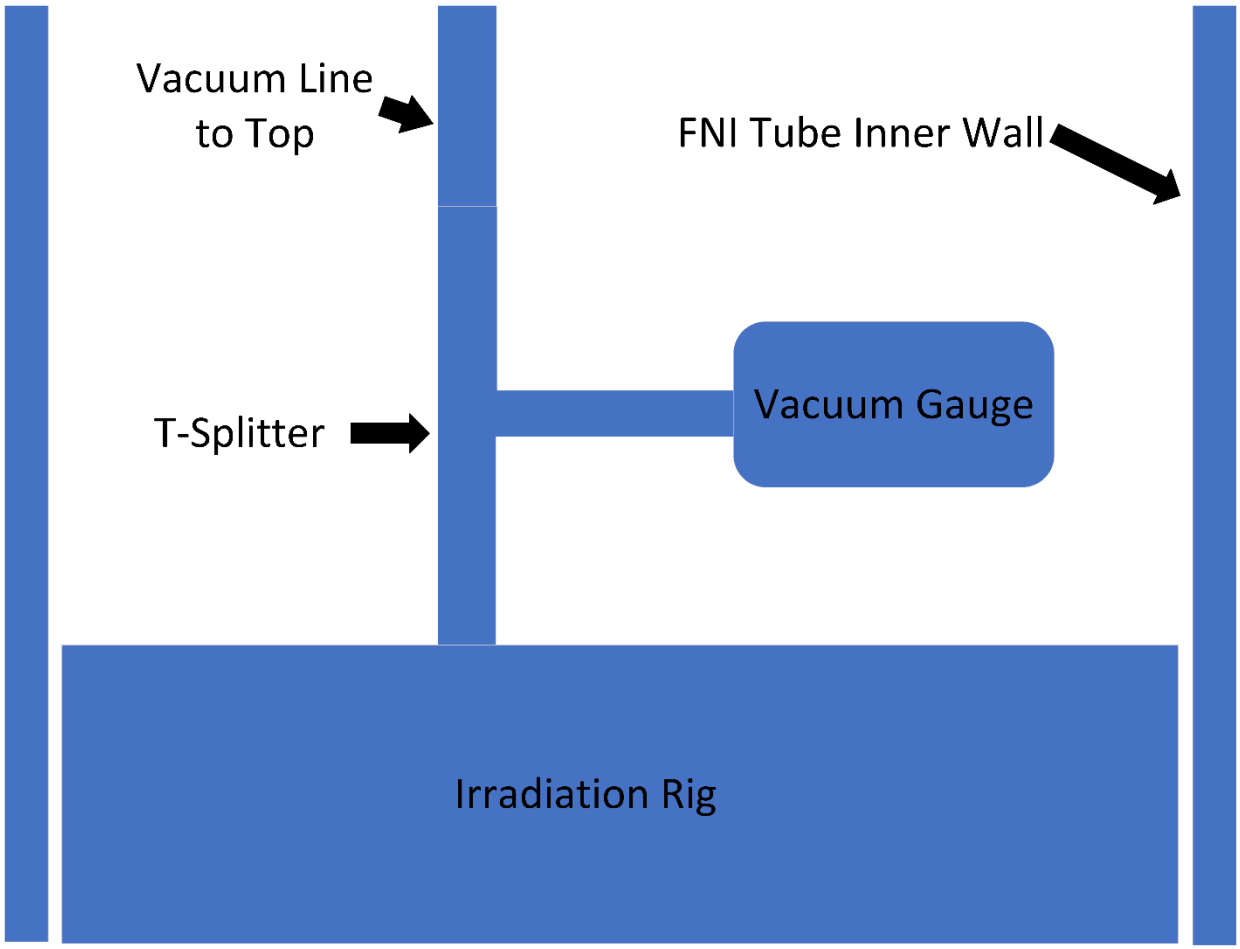

Figure 3. Vacuum System Diagram

3.4 Cryogenic Cooling System

The purpose of this facility is to understand the effects of cryogenic irradiation on materials. A cryogenic cooling system is therefore necessary to cool material samples to low temperatures. Liquid nitrogen (LN2) was chosen as the cryogen for this study (liquified form of nitrogen that has a normal boiling point of 77.36 K). Liquid hydrogen or liquid helium could also

realistically be used in the same system however heat transfer concerns would need to be investigated before use due to their lower boiling point. The two cooling method options identified for the system were a (1) cooling bath or (2) cryogenic pump.

3.4.1 Liquid Cryogen Cooling Bath

A cooling bath in the irradiation rig would involve preloading the experimental volume with cryogen before it is placed inside the FNI to be irradiated. The CRIF facility at Ohio State utilizes a main Dewar with 10 L inner volume which houses the liquid cryogen and experimental facilities. Material samples are placed in the Dewar, liquid helium or nitrogen is poured into the volume, and finally the cryostat is sealed and lowered into the 10-inch dry tube for irradiation. MCNP simulations conservatively estimated that the CRIF could operate for 6.66 hours at 15 kW reactor power before total liquid helium boil-off. During initial experimentation, the CRIF was operated for 5 hours 7 minutes with approximately 30-40% of liquid helium remaining [4]. Although this method has been demonstrated to be effective, the constraints placed on reactor operation time are limiting and a more consistent supply of cryogenic liquid is desired.

3.4.2 Liquid Cryogen Pumping System

To combat this challenge, it was determined a liquid cryogen pumping system should be used to maintain a more consistent supply of cryogen to the experimental volume of the irradiation rig. A number of challenges arise from the use of this method which center around the complexity of cryogenic liquid flow. Cryogenic flow differs from normal fluid flow due to the fact that the proportion of vapor and liquid within the flow is constantly changing. Two phase

flow is unavoidable in cryogenic systems because any heat flux into the liquid will cause boiling. In addition, any flow restriction such as fittings or elevation change will cause two phase flow [44]. Due to the anticipated complexity of cryogenic liquid flow, the cooling system will need to be designed by a cryogenic engineer to ensure proper analysis. General system features necessary for the rig will be discussed below.

Cryogenic transfer lines are intended for transferring fluids between two cryogenic devices. These lines are a necessary component of most cryogenic systems and typically consist of vacuum jacketed pipes to minimize the absorption of heat [45]. Transfer pipes are typically made of austenitic stainless steels capable of maintaining structural integrity under cryogenic temperatures.

To facilitate flow into and out of the cannister, a KF-25 liquid or gas double feedthrough flange can be used which is manufactured by Ideal Vacuum Products. The KF-25 vacuum fitting would maintain the vacuum between the inner and outer cannisters while also allowing cryogenic liquid to flow in and out of the experimental volume.

The large-scale application of cryogenic pumping has been around since the space race of the 1950s. Compact centrifugal cryogenic pumps have been demonstrated for research applications with small heads [46][47][48]. Researchers at Changwon National University were able to design and develop a partial emission type liquid nitrogen pump capable of transporting LN2 over long distances for high temperature superconductor power cables [49].

Neglecting friction losses, a minimum head of 20 feet is required to reach the bottom of the FNI tube. A robust pumping system is therefore required to maintain and control the rig's liquid nitrogen supply. Companies such as Barber Nichols, Flowserve, Nikkiso, and Cryogenic Machinery Corporation specialize in the design and manufacture of cryogenic pumps. These

products can be custom designed for integration within a specific system which would be ideal for the unique challenges associated with the cryogenic irradiation facility at the PSBR.

3.5 Design Assembly

The irradiation rig outer and inner cylinders will be manufactured out of Aluminum 6061 with a T6 temper. The inner cannister will consist of an experimental volume capable of holding a material sample and cryogenic liquid. Liquid nitrogen supply and return lines will run down the FNI tube and be connected to the inner cannister volume via a KF-25 double feed through flange. The LN2 will be pumped through the system via a liquid nitrogen pumping system. To minimize heat transfer, the outside of the inner cannister will be wrapped in MLI. Once the inner cannister has been connected to the outer cannister, the volume between the inner and outer cannisters will be evacuated to ensure proper function of the MLI. A vacuum pump will be connected to a vacuum transfer line which will run down the FNI tube. The turbopump line will be connected to the rig via a KF-25 mating flange and will also contain a vacuum gauge to monitor the system pressure. The required dimensions of each rig component will be determined in Chapter 4.

Chapter 4

Analysis

4.1 SOLIDWORKS Model

The major limiting dimension of the irradiation rig design was the inner diameter of the FNI tube. The FNI tube has an inner diameter of 10.02 inches and to ensure a sufficient gap, the irradiation rig was limited with a maximum diameter of 9.95 inches. The outermost part of the assembly is the outer cannister which is shown in Figure 4. The maximum diameter of the outer cannister occurs on the top plate, which has an outer diameter of 9.95 inches. The top plate contains four 0.2-inch diameter holes, spaced 90 degrees apart, to accommodate 1/4”-20 Grade 8 Steel Hex Head Screws. The irradiation rig will not be under significant axial stress and therefore four 1/4”-20 Grade 8 Steel Hex Head Screws will sufficiently secure the outer cannister to the lid.

The lid assembly contains the lid for the two cannisters, a KF-25 double feed through flange, and a KF-25 vacuum mating flange. The lid contains eight holes, four for each cannister, to allow for the screws to fasten the lid to each cannister. The lid assembly is shown below in Figure 5.

The inner cannister contains the same layout of 0.2-inch diameter holes as the outer cannister and is shown in Figure 6. These holes accommodate the same type of screws as the outer cannister to secure the inner cannister to the lid. The inner cannister is surrounded by a one-centimeter thick layer of MLI as shown in Figure 7. To allow for sufficient clearing between the vacuum mating flange and the MLI, the outer diameter of the inner cannister was chosen to be 3.41 inches. The goal of this project, given the size constraints of the FNI tube, was for the

irradiation rig to hold a maximum sample of 2-inch diameter and 12-inch length. To meet this requirement, the sample holder within the inner cannister has a height of 12 inches and a diameter of 2.08 inches. The diameter of the sample holder was increased slightly from the 2-inch goal to provide additional clearance for the sample to be easily loaded and unloaded from the inner cannister.

The entire rig assembly is shown in Figure 8. The model for the 1/4”-20 Grade 8 Steel Hex Head Screws and corresponding washers and nuts were taken from McMaster-Carr. The models for the KF-25 double feed through and mating flanges were taken from Ideal Vacuum Products. This irradiation rig is capable of accommodating a cylindrical material sample with a maximum diameter and height of 2 and 12 inches respectively. The KF-25 double feedthrough flange supplies liquid nitrogen to the inner cannister and material sample. The inner cannister is surrounded by a 1-centimeter thick layer of MLI to reduce heat transfer into and out of the inner cannister volume. A KF-25 vacuum mating flange allows for the attachment of a vacuum transfer line and gauge to ensure the area between the inner and outer cannisters remains at vacuum conditions. The outer cannister and lid ensure that all components and fluids are contained within the experimental vessel.

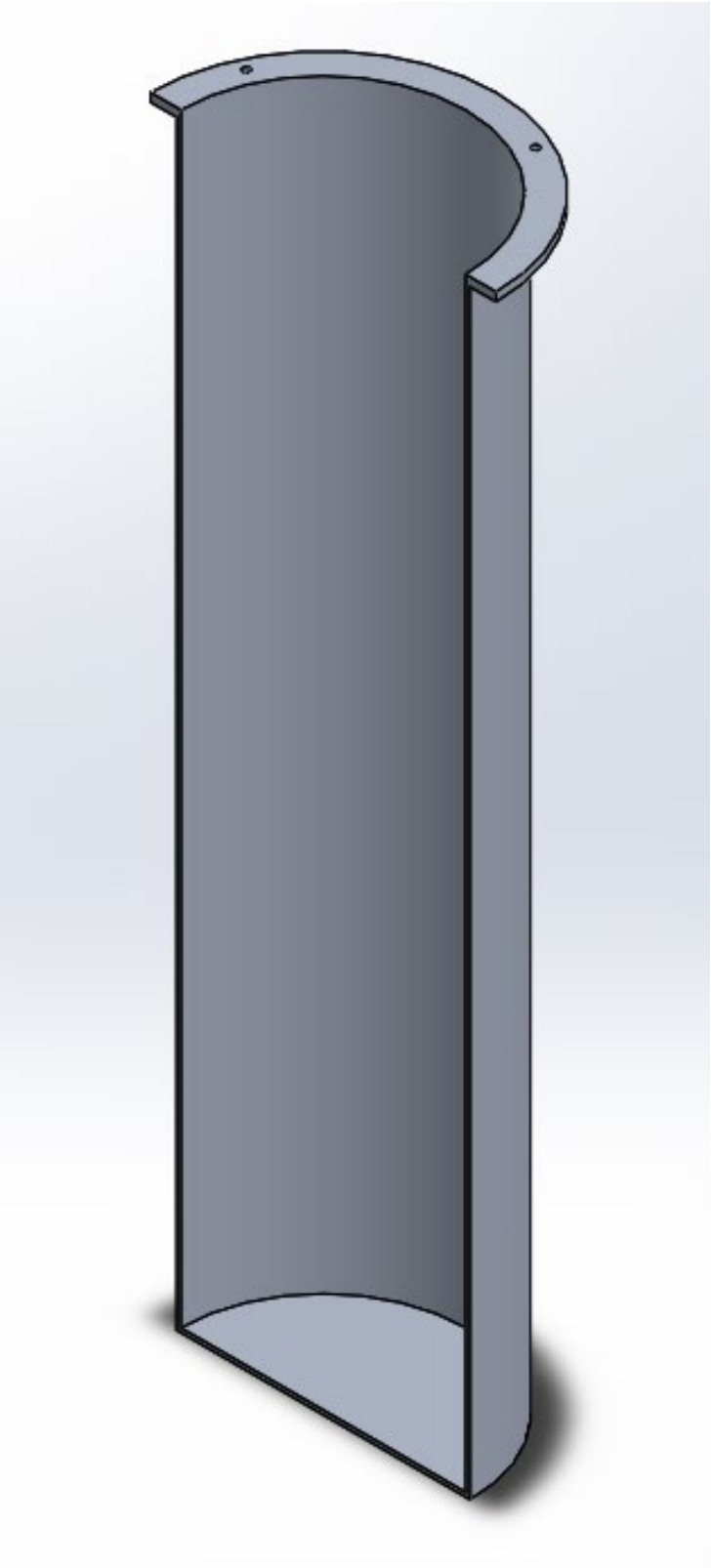

Figure 4. Outer Cannister SOLIDWORKS Model

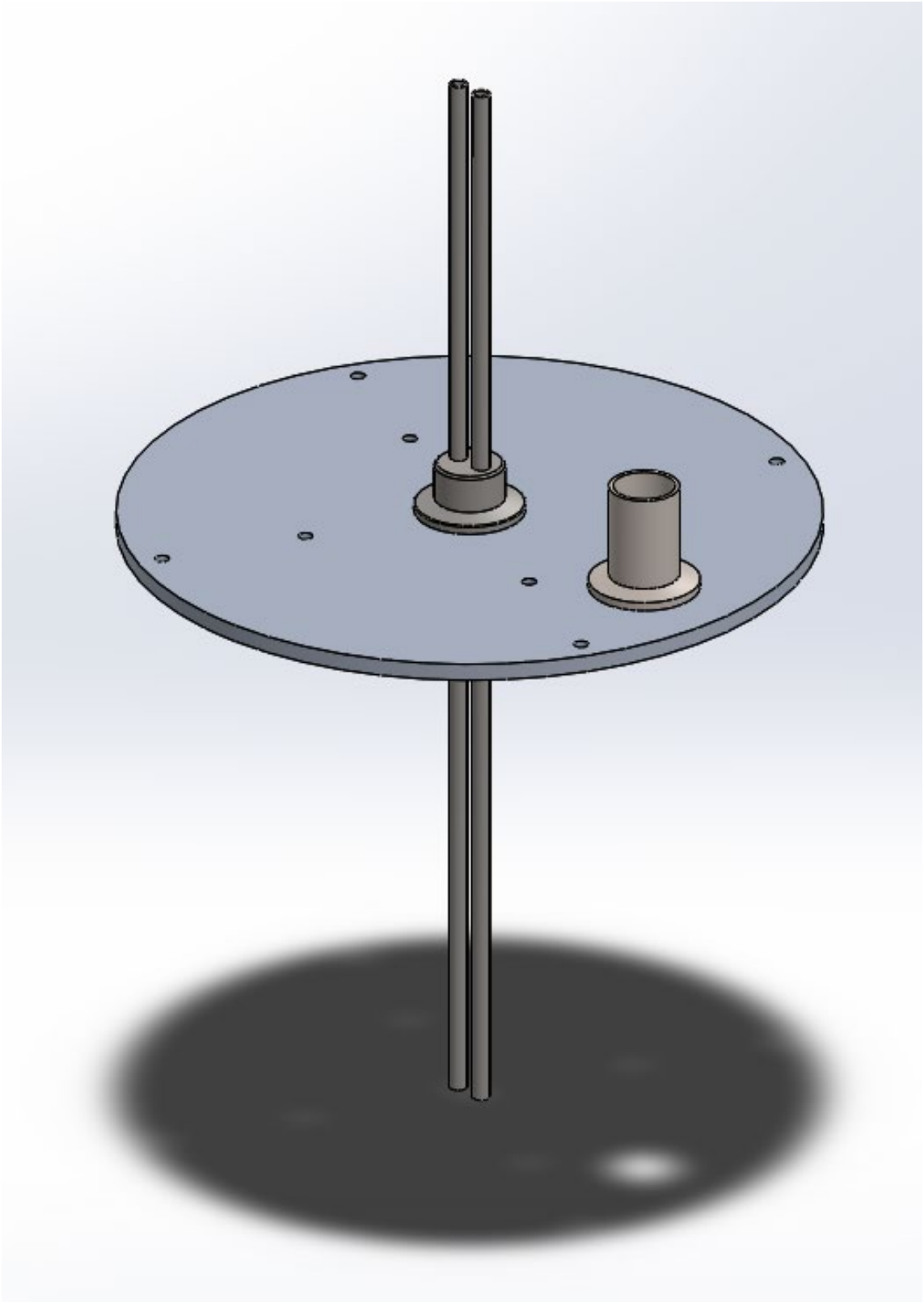

Figure 5. Lid Assembly SOLIDWORKS Model

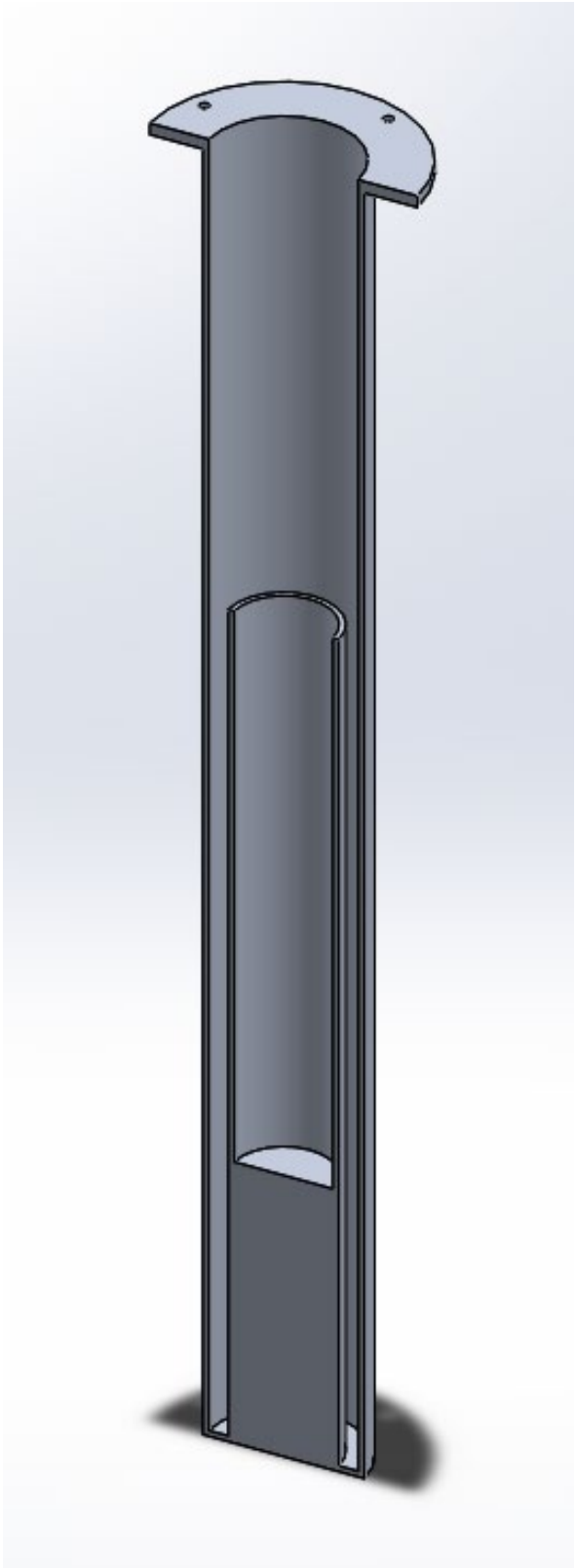

Figure 6. Inner Cannister SOLIDWORKS Model

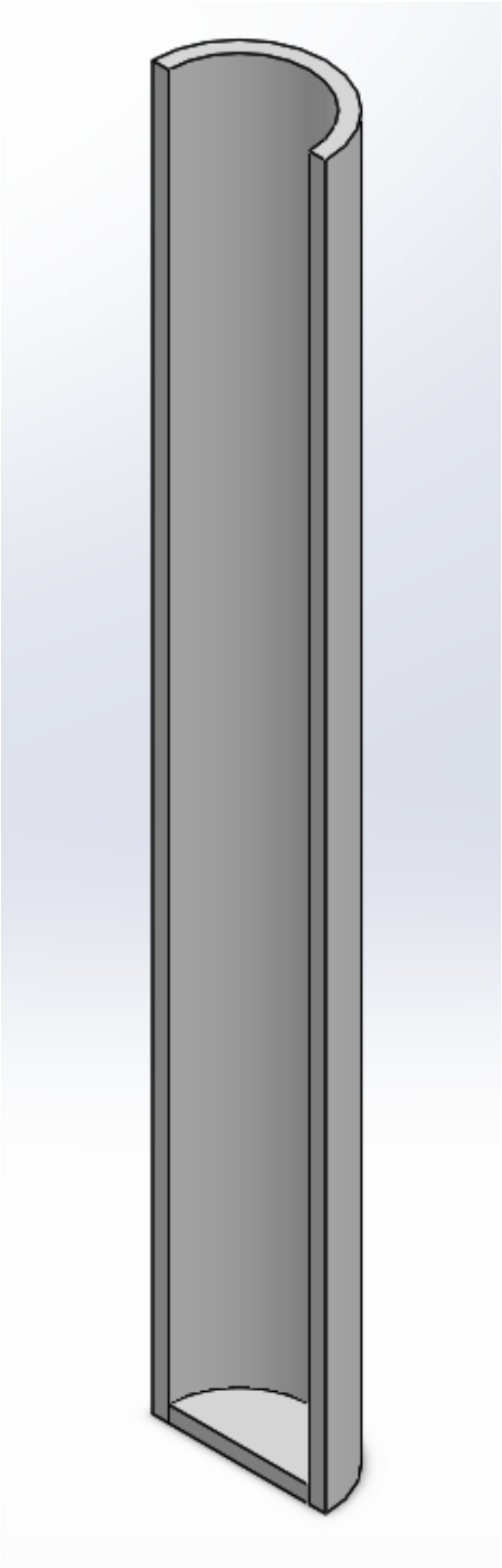

Figure 7. Multi-Layer Insulation SOLIDWORKS Model

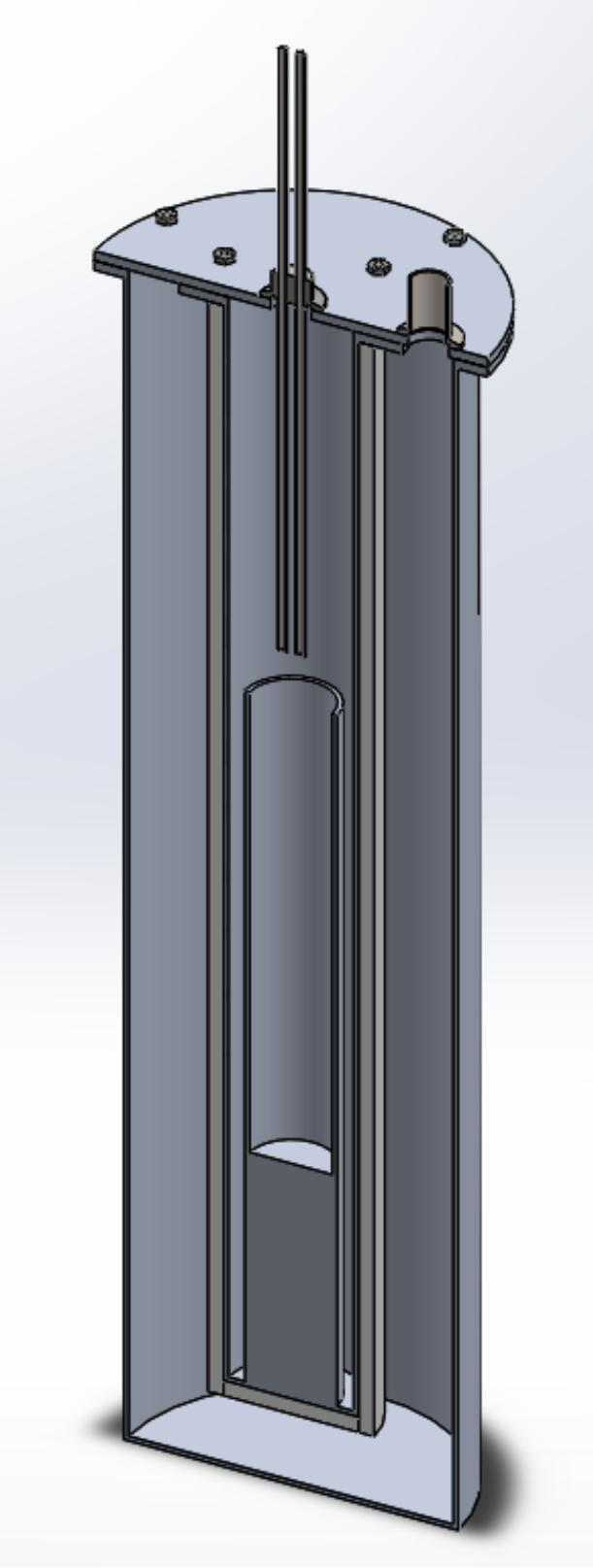

Figure 8. Cryogenic Irradiation Rig SOLIDWORKS Model

4.2 Gamma Heating

Gamma heating rates within research reactors such as the PSBR are extremely important to consider as they affect the safety and performance of the reactor. For the design of a cryogenic irradiation rig, gamma heating within the components will be crucial for determining the mass flow rate of liquid nitrogen necessary to maintain the material sample at 77 K. Although the calculation of necessary LN2 flow rate is not within the scope of this thesis, information on gamma heating within the irradiation was calculated to assist in future work.

A full-core, MCNP model of the PSBR was run with F6:p tallies to measure gamma heating in the components around the FNI tube. The MCNP F6:p tally yields track length estimates of the total energy deposition to a cell due to photon interactions. Output results are given in units of MeV/g/source particle. Tally 26 of the model corresponds to the aluminum box around the FNI tube, which provides an approximation for gamma heating rates within the aluminum irradiation rig. Tally 26 produced a gamma heating approximation of 3.6398×10^{-7} MeV/g/source particle. This was converted to a more useful unit of 4.422357×10^{-9} /g using the following stoichiometry.

$$\frac{2.43\ neutrons}{1\ fission} \times \frac{1\ fission}{200\ MeV} \times \frac{1\ MeV}{1 \times 10^{-6}\ eV} \times \frac{1\ eV}{1.602 \times 10^{-19}\ J} = 7.584 \times 10^{10}\ \frac{neutrons}{J}$$

$$\frac{3.6398 \times 10^{-7}\ MeV}{g * neutron} \times \frac{1 \times 10^{6}\ eV}{1\ MeV} \times \frac{1.602 \times 10^{-19}\ J}{eV} = 5.831 \times 10^{-20}\ \frac{J}{g * neutron}$$

$$\left[7.584 \times 10^{10}\ \frac{neutrons}{J}\right] \times \left[5.831 \times 10^{-20}\ \frac{J}{g * neutron}\right] = 4.422 \times 10^{-9} g^{-1}$$

Using this value, the gamma heating rates within the aluminum of the assembly were calculated for different reactor powers. An example calculation is shown below with a list of values at different reactor powers given in Table 1.

$$4.422 \times 10^{-9} g^{-1} \times 50 \times 10^{3}\, W = 0.000221\, W/g$$

Table 1. Gamma Heating Rates for Varying PSBR Reactor Power Levels

Reactor Power	Gamma Heating Rate (W/g)
50 kW	0.000221
100 kW	0.000442
500 kW	0.00221
1 MW	0.00442
2 GW	8.85

A steady state reactor power of 1 MW was chosen to provide a sample calculation of energy deposition within the irradiation rig. The inner cannister, outer cannister, and lid assembly were considered for gamma heating and all materials were assumed to have the same gamma heating rate as the aluminum box surrounding the FNI. The mass of each irradiation rig component was taken from the corresponding SOLIDWORKS part. The gamma energy deposition results are shown below in Table 2.

Table 2. Gamma Energy Deposition within Irradiation Rig Components

Component	Mass (g)	Gamma Energy Deposition (W)
Outer Cannister	4942.14	21.9
Inner Cannister	3427.26	15.2
Lid Assembly	1081.31	4.78

4.3 Heat Transfer

To preliminarily examine heat transfer between the rig and reactor pool water, a simplified resistance network was constructed. A schematic of the irradiation rig is shown below in Figure 9. In the figure, the inner and outer cannisters are shown in black and the multi-layer insulation is shown in gray. D1, D2, and D3 correspond to the inner cannister, insulation, and outer cannister inner walls respectively.

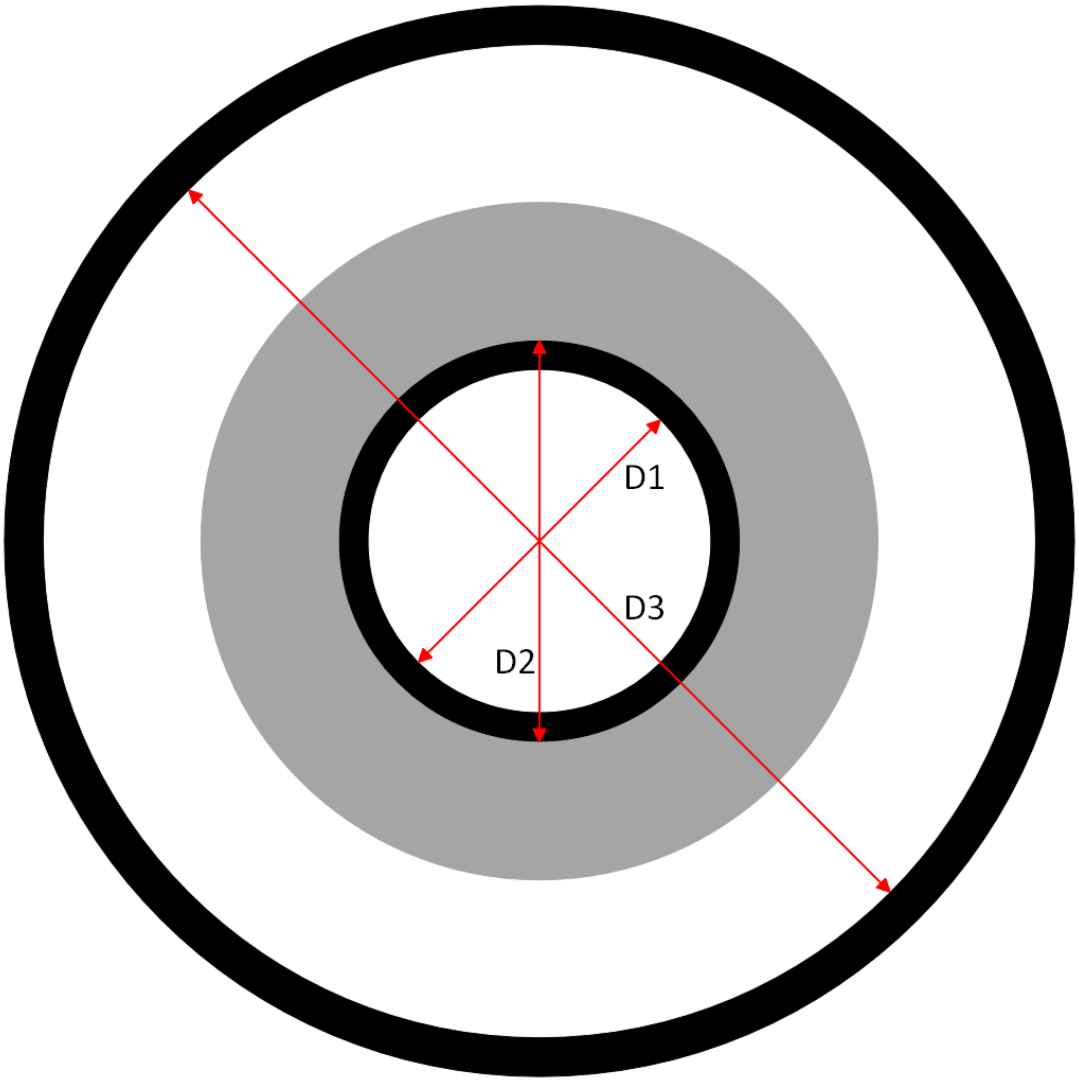

Figure 9. Irradiation Rig Drawing

As discussed in Chapter 3.3, the region between the inner and outer cannister is to be evacuated using a vacuum pumping system. A state of near vacuum will exist between the outer wall of the inner cannister and the inner wall of the outer cannister. This includes the multi-layer insulation layer which will be evacuated of residual air. Within a true vacuum, heat transfer occurs exclusively by radiation, as conduction and convection are not possible. With conduction and convection not occurring within a vast majority of the irradiation rig, the heat transfer was approximated by assuming exclusively radiant heat transfer. A network representation of the simplified analysis is shown below. The multilayer insulation, constructed from an extremely low emissivity material, was treated as a radiation shield. The FNI tube itself and surrounding shielding pedestal were not included in this network. Neglecting conduction and convection in these regions would be inaccurate and, therefore, the inner wall of the outer cannister was chosen as the outer limit of analysis.

$$q' = \frac{E_{b1} - E_{b2}}{R_{total}} = \frac{\sigma(T_1^4 - T_3^4)}{R_{total}}$$

$$R_{total} = \frac{1-\epsilon_1}{\epsilon_1(\pi D_1 L)} + \frac{1}{F_{12}(\pi D_1 L)} + 2\left[\frac{1-\epsilon_2}{\epsilon_2(\pi D_2 L)}\right] + \frac{1}{F_{23}(\pi D_2 L)} + \frac{1-\epsilon_3}{\epsilon_3(\pi D_3 L)}$$

The temperature of the inner cannister inner wall is assumed to equal to the temperature of liquid nitrogen. This is reasonable because the inner cannister wall is in constant contact with liquid nitrogen. The temperature of the outer cannister inner wall must fall between the temperature of liquid nitrogen and the bulk temperature of the reactor pool water (~293 K). Due to the effectiveness of the MLI and vacuum at minimizing heat transfer, it was estimated that the outer cannister inner wall would be 273 K. The emissivity of aluminum alloys varies greatly with surface roughness and temperature. For this problem, it was determined that the aluminum would have an approximate emissivity coefficient of 0.1. The value of emissivity for MLI also varies

with material type and was estimated to be 0.015 using literature [50][51]. These parameters are shown below in Table 3.

Table 3. Heat Transfer Properties

Part of Assembly	Temperature (K)	Diameter (m)	Emissivity
Inner Cannister Inner Wall	77.36	0.080264	0.1
Multi-Layer Insulation Inner Wall	N/A	0.086868	0.015
Outer Cannister Inner Wall	273	0.208280	0.1

The linear heat transfer rate through the irradiation rig was therefore found to be -0.177 W/m. When compared to gamma heating values calculated in Chapter 4.2, this heat transfer rate is relatively quite small. Realistically, conduction and convection will occur with the aluminum layers of the rig and within the MLI. The actual heat transfer rate within the rig is therefore greater than the calculated value. Although the assumptions made throughout the analysis are not entirely accurate, the calculated value does provide a close estimate to the rig's performance. The MLI, when combined with a vacuum, provides an excellent heat transfer barrier. When internal heat generation within the rig components due to gamma ray interactions is also considered, it is reasonable to conclude that the cryogenic fluid within the irradiation rig will not cause reactor pool water to freeze. The CRIF utilizes a similar insulation/vacuum combination design and does not freeze pool water, further confirming this analysis [4].

Chapter 5

Conclusion

The Radiation Science & Engineering Center at Penn State sought to investigate the feasibility of a cryogenic irradiation facility at the Breazeale Nuclear Reactor. An irradiation rig has been designed for use inside the FNI tube, located adjacent to the PSBR reactor core. The irradiation rig will be manufactured out of Aluminum 6061-T6 due to its excellent performance as a structural material under PSBR reactor conditions. The inner cannister contains an experimental volume capable of holding a cylindrical material sample with a maximum diameter and height of 2 and 12 inches respectively. The material will be subjected to a recirculating liquid nitrogen bath. Liquid nitrogen supply and return lines will connect to the experimental volume via a KF-25 double feed through flange. Liquid nitrogen will be continuously supplied to the system via a liquid nitrogen pumping system to allow for extended irradiations at constant temperature. To mitigate heat transfer to the reactor pool water, the inner cannister will be wrapped in a one-centimeter thick layer of multi-layer insulation. The volume between the inner and outer cannister will be evacuated to further decrease the thermal conductivity of the MLI. A vacuum turbopump line will connect the irradiation rig to a vacuum pumping system to maintain this vacuum. The rig will be preloaded with a material specimen and subsequently lowered into the FNI tube using the overhead crane located in the reactor bay. SOLIDWORKS was used to create a three-dimensional model of the rig. Technical drawings of the irradiation rig parts and their important dimensions can be found in Appendix A.

Heat transfer between the reactor pool water and cryogenic fluid was an important consideration during the design process. The rig was designed to ensure that reactor pool water would not freeze during operation. To perform a preliminary heat transfer analysis, the gamma

heating within the rig was calculated using the PSBR full-core MCNP model. At a steady state reactor power of 1 MW, the gamma heating rate within the aluminum box of the FNI tube was calculated to be 0.00442 W/g. This rate was multiplied by the mass of each part to estimate energy deposition within the rig.

Following this analysis, a simplified resistance network was constructed for the rig. The 12-inch length of the experimental volume was used as the cross section for this analysis due to its location near the center of the rig. The gradient of the heat flux at the center should be close to zero and, therefore, axial heat transfer was neglected. Due to the evacuation of the volume between the inner and outer cannisters, conduction and convection were determined to be minimal when compared to radiation as heat transfer modes within the rig. The heat transfer was therefore approximated by assuming exclusively radiant heat transfer. The linear heat transfer rate through the irradiation rig was calculated to be -0.1772 W/m. The MLI, when combined with high vacuum conditions, provides an excellent thermal resistance method. When gamma heating within the rig components is also considered, it is reasonable to conclude that the cryogenic fluid within the irradiation rig will not cause reactor pool water to freeze.

The viability of a cryogenic irradiation facility is therefore shown as described above. Cryogenic irradiation at the PSBR can be realized by utilizing an irradiation rig inside the FNI tube. Before manufacturing and use however, further analysis is required. Gamma heating rates were estimated for the rig using the MCNP tally corresponding to the aluminum box around the FNI tube. To obtain more accurate results, the irradiation rig geometry should be added to the full-core PSBR model. This will also be necessary to simulate the irradiation rig's performance during reactor operations. Accurate generation heat within each component by gamma ray irradiation will be critical to determine the flow rate of liquid nitrogen required to cool the

material sample. This consistent flow rate will ensure the experimental volume remains at a constant temperature.

In addition, an elementary heat transfer analysis was used to confirm the thermal performance of the irradiation rig. A more extensive and accurate modeling/simulation of the heat transfer between the rig and reactor pool water will need to be performed. In reality, conduction and convection cannot be ignored and the FNI tube, air gap, and surrounding shielding pedestal should be included in the analysis. A volumetric heat source due to gamma heating must also be included within this model. A three-dimensional analysis of the rig will therefore be needed to confirm that (1) the reactor pool water does not freeze and (2) the material remains at liquid nitrogen temperature. While more in-depth analysis is required, this thesis serves as an introductory study and demonstrates that a cryogenic irradiation facility at the PSBR is feasible.

Appendix A

Engineering Drawings of Irradiation Rig Components

Inner Cannister

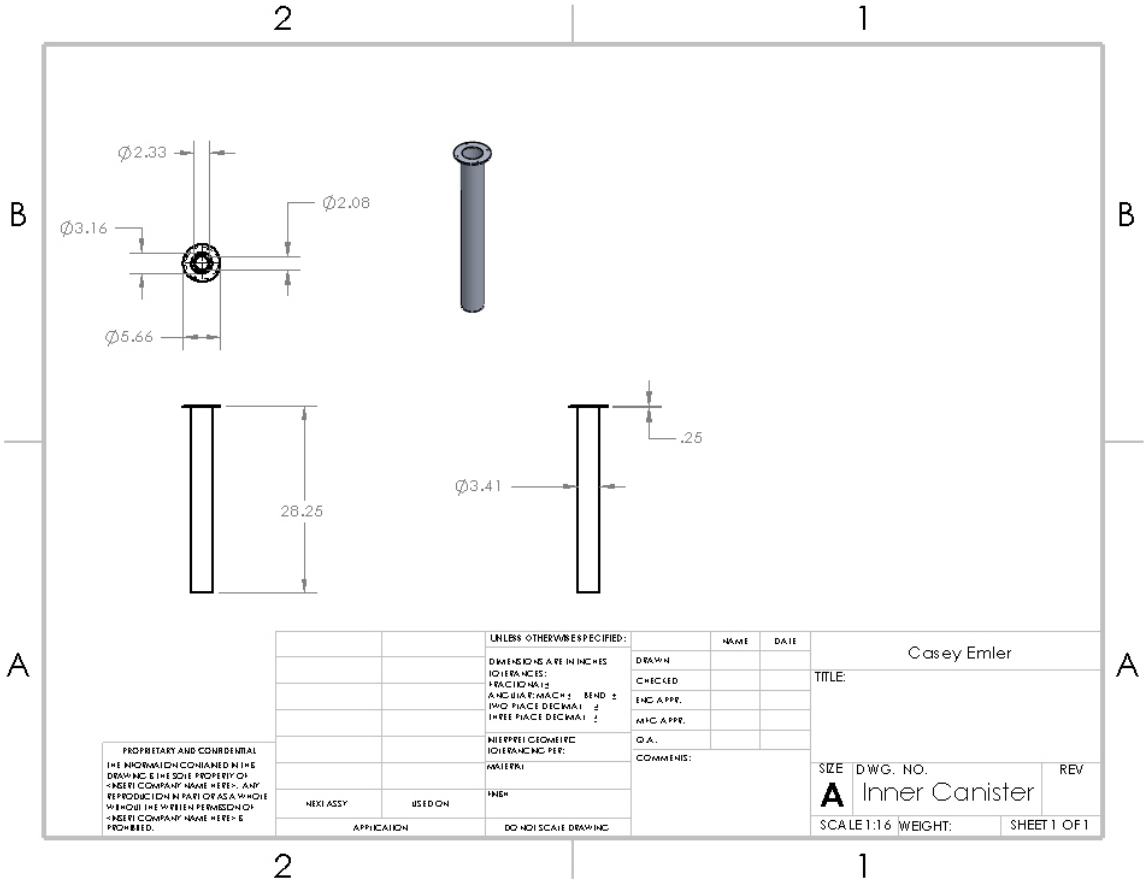

Outer Cannister

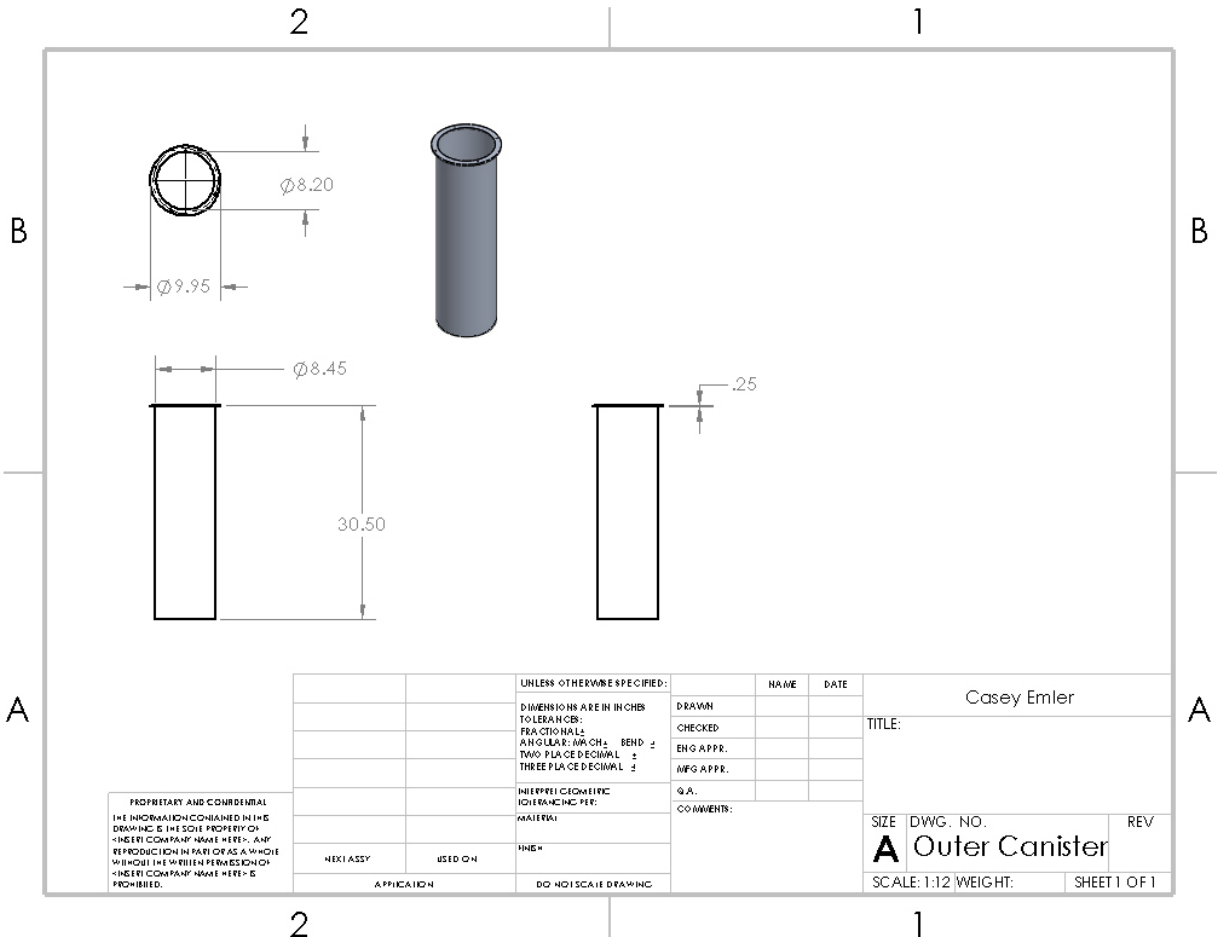

Lid Assembly

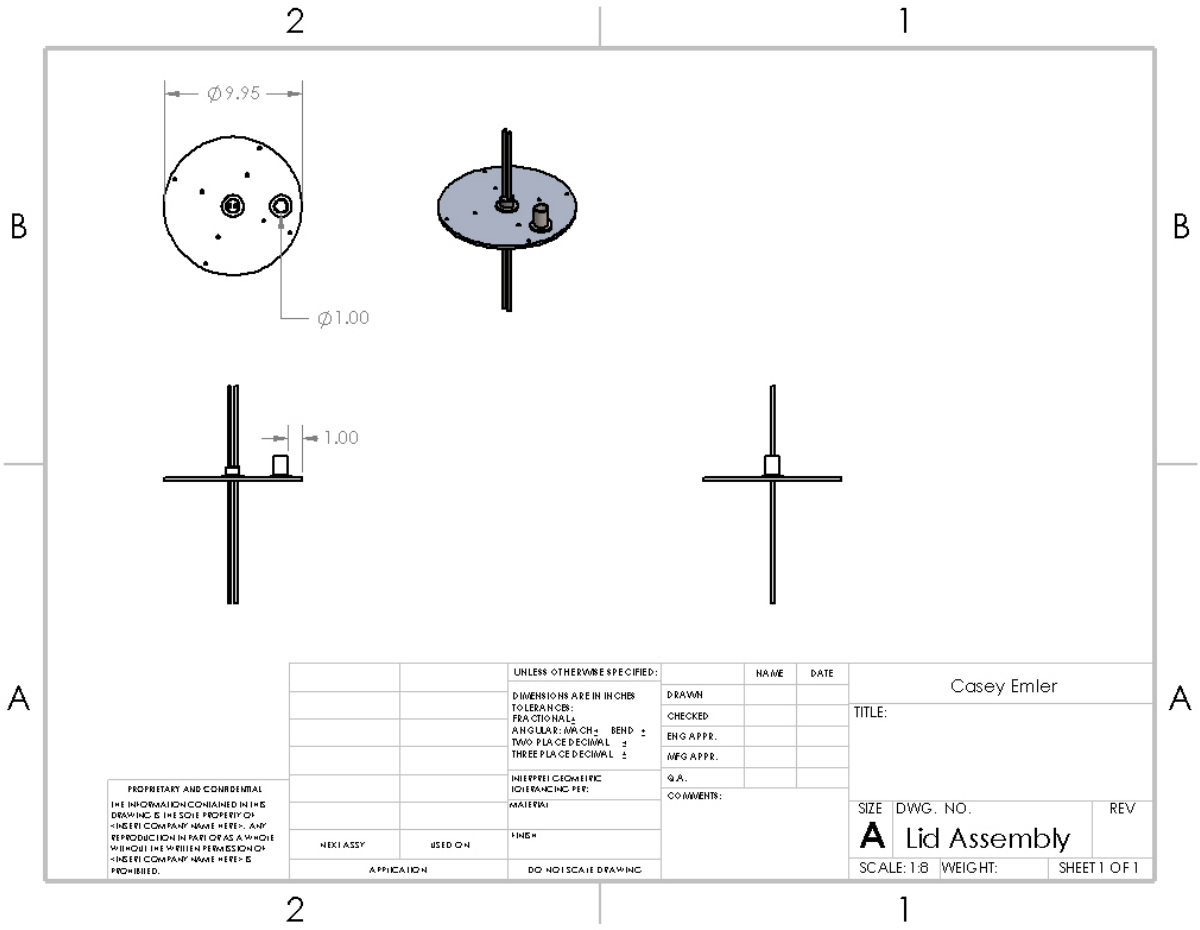

Rig Assembly

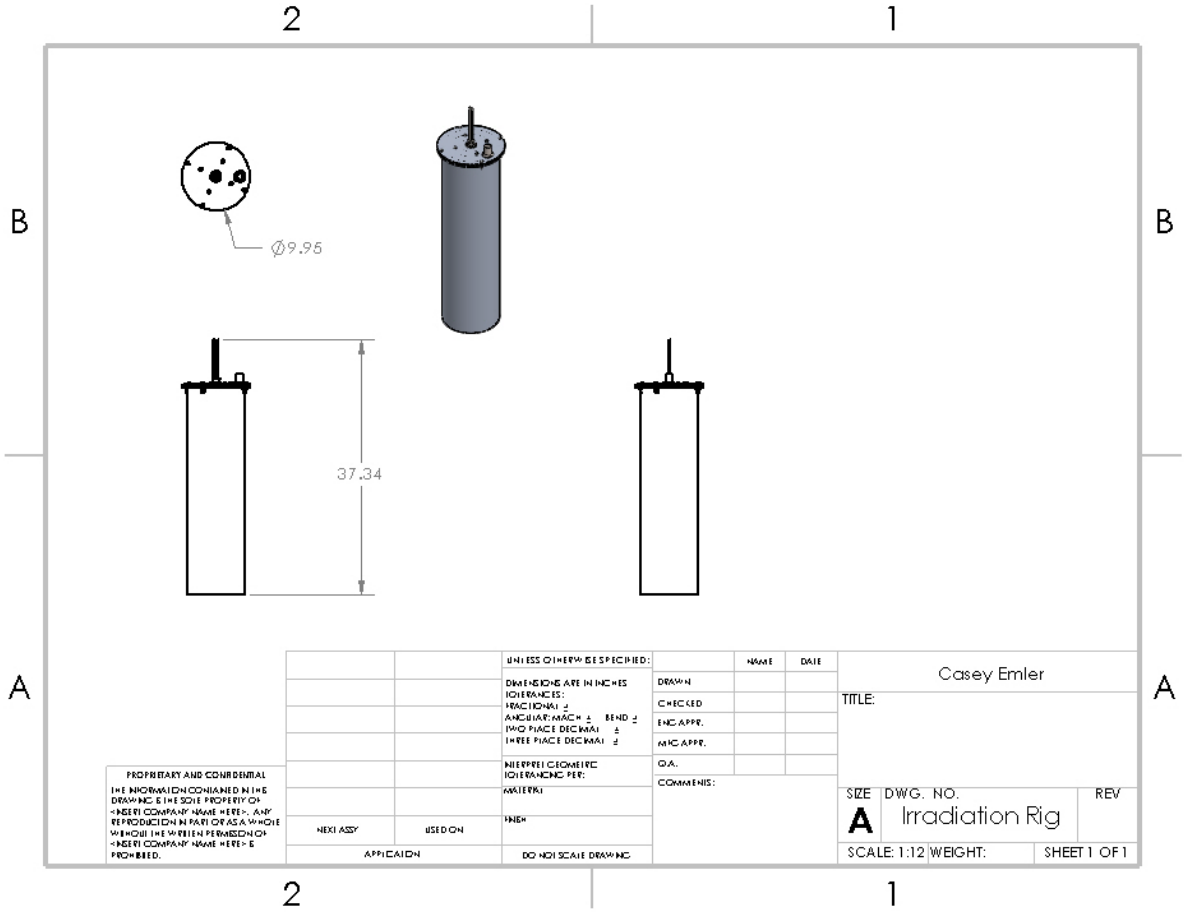

BIBLIOGRAPHY

[1] F. A. Haley and R. R. Wyer, “Irradiation System for Cryogenic Experiments in the Plum Brook Reactor,” Cleveland, Jan. 1966.

[2] M. Yoshida *et al.*, “Low-temperature neutron irradiation tests of superconducting magnet materials using reactor neutrons at KUR,” 2012, pp. 167–173, doi: 10.1063/1.4712093.

[3] J. Collot *et al.*, “A neutron irradiation facility featuring cryogenic temperatures and dedicated to Large Hadron Collider detector design,” *Nucl. Instruments Methods Phys. Res. Sect. A Accel. Spectrometers, Detect. Assoc. Equip.*, vol. 350, no. 3, pp. 525–529, Nov. 1994, doi: 10.1016/0168-9002(94)91253-X.

[4] B. Reinke, “Cryogenic Irradiation and Low Temperature Annealing of Semiconductor and Optical Materials,” The Ohio State University, 2016.

[5] D. Thomas, M. Houts, W. Walters, K. Hollingsworth, R. Frederick, and J. Cassibry, “Toward the Engineering Feasibility of the Centrifugal Nuclear Thermal Rocket,” in *72nd Internation Astronautical Congress*, 2021, pp. 1–10.

[6] J. Knaster, A. Moeslang, and T. Muroga, “Materials research for fusion,” *Nat. Phys.*, vol. 12, no. 5, pp. 424–434, May 2016, doi: 10.1038/nphys3735.

[7] M. Kiritani, T. Yoshiie, S. Kojima, Y. Satoh, and K. Hamada, “Fission-fusion correlation by fission reactor irradiation with improved control,” *J. Nucl. Mater.*, vol. 174, no. 2–3, pp. 327–351, Nov. 1990, doi: 10.1016/0022-3115(90)90245-I.

[8] R. E. Sharp, “RADIATION EFFECTS ON POWER SEMICONDUCTORS,” 1994.

[9] A. J. Leggett, “Diatomic Molecules and Cooper Pairs,” 1980.

[10] K. Osamura, *Composite Superconductors*. New York: Marcel Dekker Inc., 1993.

[11] J. Lamarsh and A. Baratta, *Introduction to Nuclear Engineering*, 3rd ed. 2001.

[12] A. Motta and D. Olander, *Light Water Reactor Materials*, vol. 1. 2017.

[13] M. T. Robinson, "Basic physics of radiation damage production," *J. Nucl. Mater.*, vol. 216, no. C, pp. 1–28, Oct. 1994, doi: 10.1016/0022-3115(94)90003-5.

[14] R. Benedek, "Spatial characteristics of displacement cascades in metals," *J. Appl. Phys.*, vol. 52, no. 9, pp. 5557–5565, 1981, doi: 10.1063/1.329541.

[15] P. Yvon and F. Carré, "Structural materials challenges for advanced reactor systems," *J. Nucl. Mater.*, vol. 385, no. 2, pp. 217–222, Mar. 2009, doi: 10.1016/J.JNUCMAT.2008.11.026.

[16] A. Rohanda, A. Waris, R. Kurniadi, S. Bakhri, P. Pardi, and D. Haryanto, "Validation and improvement of gamma heating calculation methods for the G.A. Siwabessy multipurpose reactor," *Nucl. Sci. Tech.*, vol. 31, no. 11, Nov. 2020, doi: 10.1007/s41365-020-00824-4.

[17] Y. K. Lee, J.-C. David, and H. Carcreff, "A GAMMA HEATING CALCULATION METHODOLOGY FOR RESEARCH REACTOR APPLICATION," 2001.

[18] M. Varvayanni, N. Catsaros, and M. Antonopoulos-Domis, "Evaluation of nuclear heating of small samples in a research reactor core," *Ann. Nucl. Energy*, vol. 35, no. 8, pp. 1414–1420, Aug. 2008, doi: 10.1016/J.ANUCENE.2008.01.014.

[19] R. Barron and G. Nellis, *Cryogenic Heat Transfer*. 2016.

[20] P. Lutkiewicz, B. Skoczeń, and C. Garion, "Micro-damage propagation in ultra-high vacuum seals," *Int. J. Press. Vessel. Pip.*, vol. 87, no. 4, pp. 187–196, Apr. 2010, doi: 10.1016/J.IJPVP.2009.10.002.

[21] A. Ustrzycka, "Physical Mechanisms Based Constitutive Model of Creep in Irradiated and Unirradiated Metals at Cryogenic Temperatures," *J. Nucl. Mater.*, vol. 548, p. 152851, May 2021, doi: 10.1016/J.JNUCMAT.2021.152851.

[22] H. R. Higgy and F. H. Hammad, “Effect of fast-neutron irradiation on mechanical properties of stainless steels: AISI types 304, 316 and 347,” *J. Nucl. Mater.*, vol. 55, no. 2, pp. 177–186, Feb. 1975, doi: 10.1016/0022-3115(75)90151-8.

[23] J. L. Straalsund and C. K. Day, “Effect of neutron irradiation on the elastic constants of Type 304 stainless steel,” *Nucl. Technol.*, vol. 20, no. 1, pp. 27–34, Oct. 1973, doi: 10.13182/NT73-2.

[24] B. K. Singh and V. Singh, “Effect of fast neutron irradiation on tensile properties of AISI 304 stainless steel and alloy Ti–6Al–4V,” *Mater. Sci. Eng. A*, vol. 528, no. 16–17, pp. 5336–5340, Jun. 2011, doi: 10.1016/J.MSEA.2011.03.066.

[25] C. Zheng and W. Yu, “Effect of low-temperature on mechanical behavior for an AISI 304 austenitic stainless steel,” *Mater. Sci. Eng. A*, vol. 710, pp. 359–365, Jan. 2018, doi: 10.1016/J.MSEA.2017.11.003.

[26] W. S. Park, S. W. Yoo, M. H. Kim, and J. M. Lee, “Strain-rate effects on the mechanical behavior of the AISI 300 series of austenitic stainless steel under cryogenic environments,” *Mater. Des.*, vol. 31, no. 8, pp. 3630–3640, Sep. 2010, doi: 10.1016/J.MATDES.2010.02.041.

[27] K. J. Lee, M. S. Chun, M. H. Kim, and J. M. Lee, “A new constitutive model of austenitic stainless steel for cryogenic applications,” *Comput. Mater. Sci.*, vol. 46, no. 4, pp. 1152–1162, Oct. 2009, doi: 10.1016/J.COMMATSCI.2009.06.003.

[28] K. Farrell and R. T. King, “TENSILE PROPERTIES OF NEUTRON-IRRADIATED. 6061 ALUMINUM ALLOY IN ANNEALED AND PRECIPITATION-HARDENED CONDITIONS,” 1979.

[29] H. E. McCoy and J. R. Weir, “Influence of Irradiation on the Tensile Properties of the

Aluminum Alloy 6061," *Nucl. Sci. Eng.*, vol. 25, no. 4, pp. 319–327, Aug. 1966, doi: 10.13182/NSE66-A18551.

[30] J. R. Weeks and C. J. Czajkowski, "EFFECTS OF HIGH THERMAL AND HIGH FAST FLUENCES ON THE MECHANICAL PROPERTIES OF TYPE 6061 ALUMINUM IN THE HFBR," 1989.

[31] K. Farrell, "Assessment of Aluminum Structural Materials for Service Within the ANS Reflector Vessel Advanced Neutron Source," 1995.

[32] S. Turner, "Fast Neutron Activation Analysis," *Anal. Chem.*, vol. 28, no. 9, 1956.

[33] M. C. Jo, S. Oberg, and W. McCarthy, "Material selection to reduce neutron activation in a petawatt laser target chamber," Oct. 2018, pp. 201–208, doi: 10.2351/1.5056532.

[34] R. Radebaugh and P. Bradley, "Aluminum 6061-T6 (UNS AA96061)," *NIST*, 2021. .

[35] T. Bellunato *et al.*, "Study of ageing effects in aerogel," *Nucl. Instruments Methods Phys. Res. Sect. A Accel. Spectrometers, Detect. Assoc. Equip.*, vol. 527, no. 3, pp. 319–328, Jul. 2004, doi: 10.1016/J.NIMA.2004.03.197.

[36] G. Wei, Y. Liu, X. Zhang, F. Yu, and X. Du, "Thermal conductivities study on silica aerogel and its composite insulation materials," *Int. J. Heat Mass Transf.*, vol. 54, no. 11–12, pp. 2355–2366, May 2011, doi: 10.1016/J.IJHEATMASSTRANSFER.2011.02.026.

[37] R. Liepins, L. J. Wood, D. S. Tucker, and F. W. Clinard, "Neutron irradiation effects on model compounds for epoxy and polyimide resins," *Int. J. Radiat. Appl. Instrumentation. Part C. Radiat. Phys. Chem.*, vol. 36, no. 3, pp. 383–391, Jan. 1990, doi: 10.1016/1359-0197(90)90023-B.

[38] R. Benaroya, T. H. Blewitt, J. M. Brooks, and C. Laverick, "Effect of fast neutron irradiation atlow temperature on nbzr coil performance," *IEEE Trans. Nucl. Sci.*, vol. 14,

no. 3, pp. 383–385, 1967, doi: 10.1109/TNS.1967.4324585.

[39] A. Nishimura *et al.*, “Irradiation effect of 14 MeV neutron on interlaminar shear strength of glass fiber reinforced plastics,” in *AIP Conference Proceedings*, Mar. 2006, vol. 824 I, pp. 241–248, doi: 10.1063/1.2192357.

[40] R. Coston and G. Vliet, “Thermal Energy Transport Characteristics along the Laminations of Multilayer Insulations,” in *Thermophysics of Spacecraft and Planetary Bodies: Radiation Properties of Solids and the Electromagnetic Radiation Environment in Space*, New York: American Institute of Aeronautics and Astronautics, 1967, pp. 909–923.

[41] M. Moser, C. Ranzenberger, and S. Duzellier, “Space environmental testing of novel candidate materials for multilayer insulation,” *J. Spacecr. Rockets*, vol. 53, no. 6, pp. 1034–1040, 2016, doi: 10.2514/1.A33487.

[42] B. D. Taylor, J. Caffrey, A. Hedayat, J. Stephens, and R. Polsgrove, “Cryogenic fluid management technology development for nuclear thermal propulsion,” 2015, doi: 10.2514/6.2015-3957.

[43] Y. Inaba, K. Tsuchiya, T. Shikama, A. Nishimura, and H. Kawamura, “Feasibility study on cryogenic irradiation facility in JMTR,” *Fusion Eng. Des.*, vol. 86, no. 2–3, pp. 134–140, Mar. 2011, doi: 10.1016/J.FUSENGDES.2010.09.024.

[44] technifab Products, “Cryogenic Liquid Flow,” *technifab Products*, 2022. .

[45] J. Fydrych, *Cryogenic Transfer Lines*. SpringerLink, 2016.

[46] D. Chopra and H. Babb, “Inexpensive liquid nitrogen pump,” *Rev. Sci. Instrum.*, vol. 46, no. 8, pp. 1126–1127, 1975, doi: 10.1063/1.1134371.

[47] G. Li *et al.*, “A compact cryogenic pump,” *Cryogenics (Guildf).*, vol. 75, pp. 35–37, Apr. 2016, doi: 10.1016/J.CRYOGENICS.2015.12.006.

[48] T. Haruyama and R. Yoshizakis, “A miniature centrifugal pump for an automatic liquid nitrogen filling system,” 1986.

[49] J. Lee, Y. Kwon, C. Lee, J. Choi, and S. Kim, “Design of Partial Emission Type Liquid Nitrogen Pump,” *Prog. Supercond. Cryog.*, vol. 18, no. 1, pp. 64–68, 2016.

[50] M. Kanda, K. Matsumoto, and S. Yamaguchi, “Heat transfer through multi-layer insulation (MLI),” *Phys. C Supercond. its Appl.*, vol. 583, p. 1353799, 2021, doi: 10.1016/j.physc.2020.1353799.

[51] T. H. Takeshi Miyakita, Ryuta Hatakenaka, Hiroyuki Sugita, Masanori Saitoh, “Evaluation of Thermal Insulation Performance of a New Multi-Layer Insulation with Non-Interlayer-Contact Spacer,” *45th Int. Conf. Environ. Syst.*, no. July, p. ICES-2015-220, 2015.

ACADEMIC VITA

EDUCATION

The Pennsylvania State University — University Park, PA
College of Engineering — May 2022
Bachelor of Science in Nuclear Engineering — Schreyer Honors College

EXPERIENCE

Nuclear Regulatory Commission — Rockville, MD/King of Prussia, PA
Nuclear Engineering Intern/Co-Op — May 2021 - Present

- Provided technical and administrative support in the agency's implementation of the Reactor Oversight Program (ROP).
- Analyzed emergency diesel generator failure instances over the past twenty years to determine important themes/trends.
- Participated in IP 64704 inspection at Oyster Creek Generation Station to assess whether the licensee has an effective decommissioning fire protection program.
- Participated in IP 71152 inspection at Peach Bottom Atomic Power Station to assess licensee response to failure of motor operated valve in the residual heat removal system.

Schreyer Undergraduate Thesis — State College, PA
Breazeale Nuclear Reactor — Fall 2021 – Spring 2022

- Purpose: Development of an irradiation rig for use inside the fast neutron irradiation tube to be used for space-based research.
- Perform heat transfer calculations to verify that the irradiation rig is held at cryogenic temperatures while also ensuring water in the reactor pool does not freeze.
- Design irradiation rig model using the SolidWorks computer aided design program.

NASA CNTR Project — State College, PA
Project Team Member — Spring 2022

- Purpose: Perform neutronics design optimization for NASA's Centrifugal Nuclear Thermal Rocket propulsion concept with the intended application of deep space travel.
- Utilizing OpenMC, Linux, Python, and optimization software to study system mass, power peaking factors, fuel and moderator temperature reactivity coefficients, etc.

Pennsylvania Department of Transportation — Harrisburg, PA
Engineering Intern — May 2019 – August 2019

- Participated in the inspection, materials testing, and completion of documentation associated with highway and bridge construction projects.
- Completed daily reports on inspection of construction and protection of environment.
- Collaborated with civil engineers daily to ensure construction was being performed according to plans and specifications.

CAMPUS INVOLVEMENT

Theta Delta Chi – Sigma Triton
Treasurer — August 2020 – December 2021

- Managed roughly $180,000 semester budget.
- Collected and deposited money into accounts, disbursed funds from accounts to pay bills and invoices, kept records of collections and disbursements, and ensured all accounts were balanced.

THON Donor Alumni Relations Chair — August 2020 - Present

- Responsible for reaching out to alumni and corporate sponsors to build relationships in the hopes that donors will continue to give financial support each year.

American Nuclear Society — April 2021 - Present

- Alpha Nu Sigma National Honor Society member.